

Characterisation of human gait using a continuous-wave radar at 24 GHz

C. Hornsteiner and J. Detlefsen

Technische Universität München, Lehrstuhl für Hochfrequenztechnik, Fachgebiet Hochfrequente Felder und Schaltungen, 80333 München, Germany

Abstract. Human locomotion consists of a complex movement of various parts of the body. The reflections generated by body parts with different relative velocities result in different Doppler shifts which can be detected as a superposition with a Continuous-Wave (CW) Radar. A time-frequency transform like the short-time Fourier transform (STFT) of the radar signal allows a representation of the signal in both time- and frequency domain (spectrogram). It can be shown that even during one gait cycle the velocity of the torso, which constitutes the major part of the reflection, is not constant. Further a smaller portion of the signal is reflected from the legs. The velocity of the legs varies in a wide range from zero (foot is on the ground) to a velocity which is higher than that of the torso. The two dominant parameters which characterise the human gait are the step rate and the mean velocity. Both parameters can be deduced from suitable portions of the spectrogram. The statistical evaluation of the two parameters has the potential to be included for discrimination purposes either between different persons or between humans and other moving objects.

1 Human gait analysis

The human gait was investigated for a long time beginning in the nineteenth century under scientific considerations. With the upcoming improvements in photography it was possible to analyse the movement of different body parts with a series of pictures. In our days the photo camera was replaced by a CCD camera and with several viewpoints from different angles it is possible to extract 3-dimensional data of the scene. A model which used such a motion capture system has been developed by Zonghua and Troje (2004). To get pe-

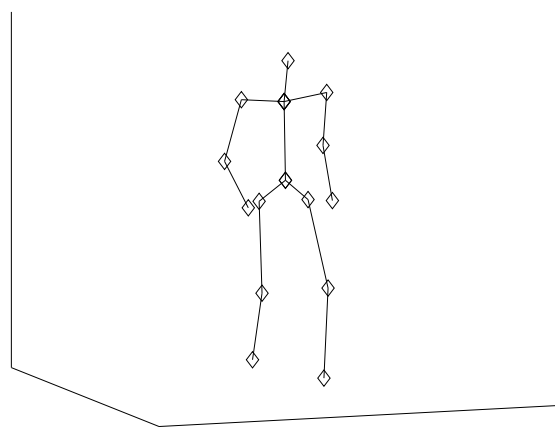


Fig. 1. Gait model of Zonghua and Troje (2004) with 15 points.

riodic data the test persons were placed on a treadmill. For identification of different body parts for the later processing each persons wore 15 reflective markers (s. Fig. 1). The 3-dimensional position was then expressed in a Fourier series

$$p(t) = p_0 + p_1 \sin(\omega t) + q_1 \cos(\omega t) + p_2 \sin(2\omega t) + q_2 \cos(2\omega t) \quad (1)$$

for each coordinate axis x , y and z . With this representation it is easily possible to look at the process from every viewpoint. To get a velocity representation of the movement Eq. (1) has to be derived. This can be done either analytically by taking the derivative from each summand or numerically by taking the derivative of the discretised time data of $p(t)$. The largest velocity components arise in the direction of locomotion. Therefore, this direction is of main interest for the measurement with a radar sensor. The obtained velocity over time for all 15 marker points is displayed in Fig. 2.



Correspondence to: C. Hornsteiner
(christoph.hornsteiner@tum.de)

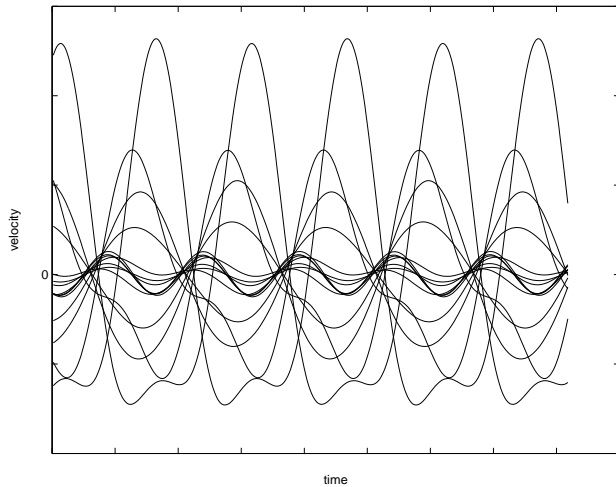


Fig. 2. Velocity in the direction of locomotion of all 15 markers over time.

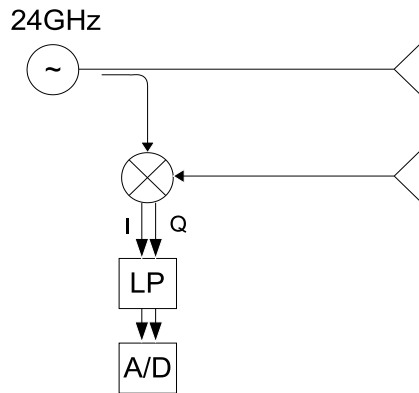


Fig. 3. Block diagram of a CW-Radar with I/Q-Demodulation.

Although the treadmill is running with constant velocity, the velocity of the torso is not constant. It is changing nearly sinusoidal with the step frequency. The highest velocities are expectedly observed from the legs. While one leg attains its maximum velocity the other is in its minimum. The velocity contribution of the knees and arms lies in between torso and legs.

2 Doppler radar

For the measurements a CW-Radar at a carrier frequency of 24 GHz was used. With the Doppler formula

$$f_D = 2f_c \frac{v}{c} \quad (2)$$

it can be seen that velocity v is proportional to the measured frequency f_D . Because of increasing Doppler frequencies

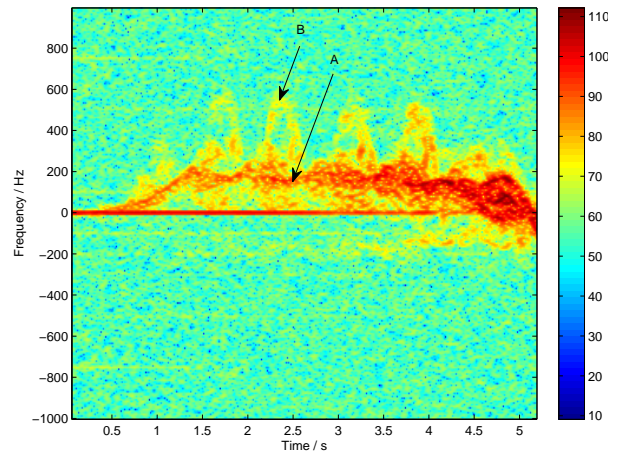


Fig. 4. Spectrogram of a walking person (window length 128 ms).

f_D with increasing carrier frequency f_c at constant velocity, the choice of a high carrier frequency leads to a better velocity resolution for a constant time interval. The basic block diagram of the radar sensor can be seen in Fig. 3. With the use of a I/Q-demodulation it is possible to discriminate between positive and negative frequencies and therefore between approach and receding motion. A spectral transform is used to derive the frequency and so the velocity. By doing this with the complete time signal the best frequency resolution is obtained giving no time resolution. In the short-time Fourier transform (STFT) only parts of the signal are transformed to frequency domain subsequently applying a windowing function $w(t)$ which is moved over the time signal $x(t)$.

$$\text{STFT}(\tau, f) = \int_{-\infty}^{+\infty} x(t) \cdot w(t - \tau) \cdot \exp(-j2\pi ft) dt$$

The so called spectrogram are the absolute values of the STFT displayed on a logarithmic scale.

3 Feature extraction

The spectrogram of a measured motion can be seen in Fig. 4. The spectral amplitude corresponds to the radar cross section of the moving parts. The main contribution (A) comes from the torso, but since it is non-rigid there is no distinct line but a spectral spread. The contribution of the legs (B) is much smaller but it can be seen that it is still above noise level. The visible velocity response of the legs is in accordance to the model. Lower frequency components occur while one foot is on the ground and the other reaches its maximum. The velocity of the torso movement (A) may be detected by taking the frequency at which the maximum amplitude occurs. Due to the spectral spread this curve will include errors if the

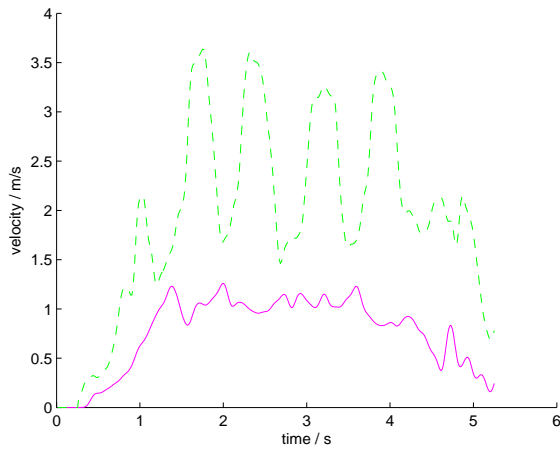


Fig. 5. Extracted velocity pattern of torso (-) and legs (- -).

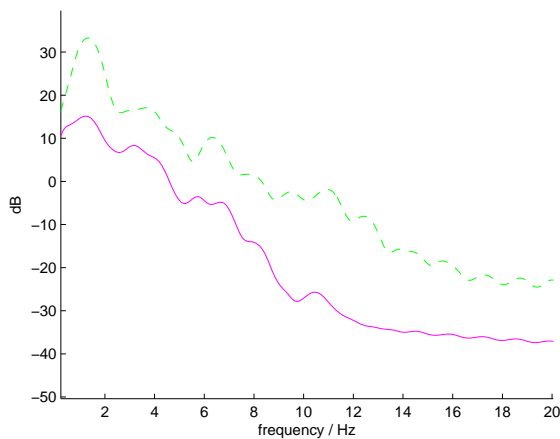


Fig. 6. Spectrum of velocity pattern from torso (-) and legs (- -).

detected velocity is not identical to the mean velocity of the torso.

The spectral components of the moving legs (B) above the torso are surrounded mostly by noise. Detection of signal above noise level is the standard process in signal theory. The resulting velocity patterns for torso and legs are displayed in Fig. 5. In both graphs the step frequency is visible. The legs with a high velocity deviation and the torso with lower velocity deviation and also visible error. For the robust detection of periodic oscillations it will be changed from time domain to frequency domain. To avoid low frequency components from acceleration process a high pass filter is applied to the signal. The resulting spectrum is shown in Fig. 6. As expected the magnitude at the step frequency of 1.3 Hz is for the legs more than 10 dB higher than those of the torso. Consequently the leg movement will be used for further evaluation.

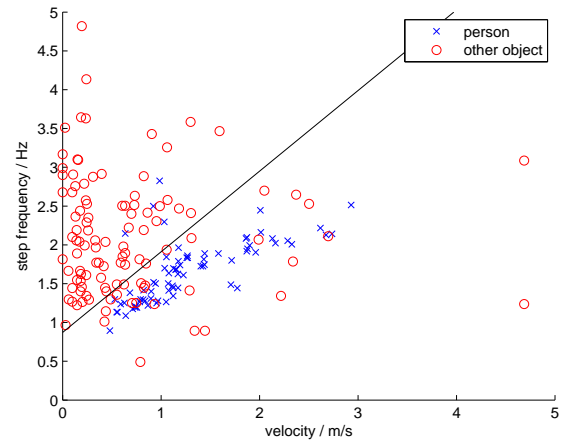


Fig. 7. Scatterplot with linear decision boundary.

Table 1. Confusion matrix with actual classes (I: Person, II: Other object) as columns and predicted classes as rows for linear discrimination.

	I	II
I	0.385	0.143
II	0.022	0.450

4 Statistical evaluation

Due to the periodic nature the step frequency is a feature candidate for a statistical evaluation. Because of known dependencies between step frequency and velocity for human gait, it is expected to be useful to combine these both features. Other objects which also produce a Doppler spectrum will not show these dependencies and should not be localized in the feature space. For discrimination two classes are created with class one including all walking persons and class two including all other objects. Class one consists of 74 data points and class two of 108 data points. The scatter plot shows a localisation of class one which makes it possible to separate both classes. The easiest way to do this is to construct a linear separation boundary using methods of linear discrimination analysis. The scatterplot with the decision boundary can be seen in Fig. 7 and the resulting confusion matrix in Table 1. The reclassification misclassification rate with this trained classifier is 16.5%. The linear classifier is not able to discriminate between points of class two lying below the localized class one. This can be improved by the construction of a nonlinear classifier. A widely used method to do this is the use of support vector machines (SVM). The nonlinearity is obtained with the use of nonlinear kernel functions. The kernel functions used here were radial basis functions. The resulting decision boundary with this classifier can be seen in

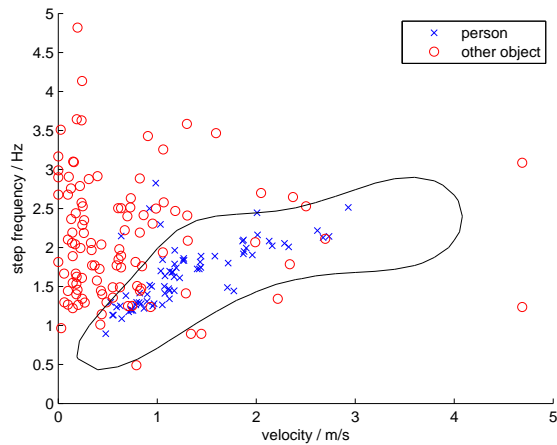


Fig. 8. Scatterplot with nonlinear decision boundary.

Table 2. Confusion matrix with actual classes (I: Person, II: Other object) as columns and predicted classes as rows for discrimination with SVM.

	I	II
I	0.385	0.088
II	0.022	0.505

Fig. 8 and in Table 2 the associated confusion matrix. With this classifier the resubstitution misclassification rate sinks to 11%.

5 Summary

The movement of different body parts can be made visible with a short-time Fourier transform of a CW radar signal. From this display it is possible to extract different velocity curves. The main parameters describing the human gait are step rate and mean velocity which could be obtained from this curves. The two dimensional scatter plot of these two features shows the possibility to discriminate between human gait and other objects. This discrimination was first done by a linear classifier and then improved with a nonlinear classifier using support vector machines.

References

- Fölster, F., Rohling, H., and Ritter, H.: Observation of a walking pedestrian with a 24GHz automotive radar sensor, GeMiC 2006, Session 10b-4, 2006.
- Gandhi, T., Gandhi, T., and Trivedi, M. M.: Pedestrian Protection Systems: Issues, Survey, and Challenges, Intelligent Transportation Systems, IEEE Transactions, 8, 413–430, 1524–9050, 2007.
- Geisheimer, J. L., Marshall, W. S., and Greneker, E.: A continuous-wave (CW) radar for gait analysis, in: Signals, Systems and Computers, 2001, Conference Record of the Thirty-Fifth Asilomar Conference, 1, 834–838, 2001.
- Otero: Application of a continuous wave radar for human gait recognition, The MITRE Corporation, 2005.
- Zonghua, Z. and Troje, N. F.: 3D Periodic Human Motion Reconstruction from 2D Motion Sequences, in: Computer Vision and Pattern Recognition Workshop, 2004 Conference, pp. 186–186, 2004.